JOURNAL OF MATHEMATICAL ANALYSIS AND APPLICATIONS **202,** 538–554 (1996)
ARTICLE NO. 0333

Irrotational, Annular Liquid Jets

Juan I. Ramos*

Departamento de Lenguajes y Ciencias de la Computación,
E. T. S. Ingenieros Industriales, Universidad de Málaga, Plaza El Ejido, s/n,
29013-Málaga, Spain

Received October 18, 1994

Perturbation methods are used to derive the asymptotic equations that govern the fluid dynamics of steady and unsteady, incompressible, inviscid, axisymmetric, irrotational, annular liquid jets employing as small parameter the slenderness ratio.

1. INTRODUCTION

The study of the steady fluid dynamics of annular liquid jets dates back to Boussinesq [1, 2], Lance and Perry [3], Hopwood [4], Taylor [5], Baird and Davidson [6], Binnie and Squire [7], and Dumbleton [8] who considered thin jets and assumed that the pressure was uniform throughout the jet while the velocity components normal and tangential to the jet's mean radius were assumed to be functions of the coordinate along the jet's mean radius. The models derived by these authors are essentially hydraulic and are only valid for thin, annular jets, i.e., jets whose thickness is much smaller than the radii of curvature of the annular liquid jet. The equations derived by Boussinesq [1, 2] were projected onto a cylindrical, polar coordinate system by Hoffman *et al.* [9] and Ramos [10]. The latter also obtained analytical solutions for long jets, i.e., jets whose mean radius at the nozzle exit is much smaller than the distance from the nozzle exit to the axial location at which the annular jet becomes a solid one. This distance is referred to as the convergence length.

* E-mail address: jirs@tecma1.ctima.uma.es.

0022-247X/96 $18.00

A hydraulic model of thin, annular liquid jets was derived by the author [11] who integrated the continuity and Euler equations along the jet's thickness and applied the kinematic and boundary conditions at the jet's interfaces where the normal velocity component is continuous while the pressure jump at the interfaces is balanced by surface tension. Although this hydraulic model has produced good agreement with experimental data [12], the assumptions of uniform pressure throughout the jet and axial and radial velocity components independent of the radial coordinate may not be justified.

In this paper, the fluid dynamics of both steady and unsteady, inviscid, irrotational, incompressible, axisymmetric, annular liquid jets are analyzed by means of perturbation methods based on the jet's slenderness ratio. (The slenderness ratio is here defined as the ratio of the jet's mean radius at the nozzle exit to the convergence length.) The analysis presented in this paper is a long-wave expansion valid for long annular liquid jets of arbitrary thickness and considers surface tension at the jet's interfaces and gravity.

Depending on the magnitude of the Weber number, i.e., the ratio of inertia to surface tension, the dynamics of annular liquid jets may be controlled by inertia or capillarity. Both inertia- and capillarity-dominated annular liquid jets are considered in the paper.

2. UNSTEADY, SLENDER, ANNULAR LIQUID JETS

The fluid dynamics of unsteady, axisymmetric, incompressible (constant density) inviscid, irrotational, annular liquid jets is governed by the velocity potential, ϕ^*, which satisfies the Laplace equation, i.e.,

$$\frac{\partial^2 \phi^*}{\partial z^{*2}} + \frac{1}{r^*}\frac{\partial}{\partial r^*}\left(r^* \frac{\partial \phi^*}{\partial r^*}\right) = 0, \tag{1}$$

where the asterisk denotes dimensional quantities, and r^* and z^* are the radial and axial coordinates, respectively.

Equation (1) is subject to the following kinematic and dynamic boundary conditions at the annular liquid jet's interfaces

$$\frac{\partial \phi^*(R_i^*, z^*, t^*)}{\partial r^*} = \frac{\partial \phi^*(R_i^*, z^*, t^*)}{\partial t^*} + \frac{\partial \phi^*(R_i^*, z^*, t^*)}{\partial z^*}\frac{\partial R_i^*}{\partial z^*}, \quad i = 1, 2, \tag{2}$$

$$p_1^* - p^*(R_1^*, z^*, t^*) = \sigma^* \left(\frac{1}{R_1^* \left(1 + \left(\partial R_1^*/\partial z^*\right)^2\right)^{1/2}} - \frac{\partial^2 R_1^*/\partial z^{*2}}{\left(1 + \left(\partial R_1^*/\partial z^*\right)^2\right)^{3/2}} \right) \tag{3}$$

$$p^*(R_2^*, z^*, t^*) - p_2^* = \sigma^* \left(\frac{1}{R_2^* \left(1 + \left(\partial R_2^*/\partial z^*\right)^2\right)^{1/2}} - \frac{\partial^2 R_2^*/\partial z^{*2}}{\left(1 + \left(\partial R_2^*/\partial z^*\right)^2\right)^{3/2}} \right), \tag{4}$$

where R_1^* and R_2^* are the radii of the jet's inner and outer interfaces, respectively, p^* is the pressure, σ^* is the liquid's surface tension, and p_1^* and p_2^* denote the pressure of the gases enclosed by and surrounding, respectively, the annular liquid jet. The gases enclosed by and surrounding the annular liquid jet will be assumed to be dynamically passive, i.e., p_1^* and p_2^* will be assumed to be spatially uniform, since their density is, in general, much smaller than that of liquids.

In addition, initial conditions and boundary conditions at $z^* = 0$, i.e., at the nozzle exit, are to be provided. The boundary conditions must be obtained by matching the potential flow inside the nozzle with that of the free, annular jet. Since the flow inside the nozzle must satisfy the no-penetration condition at the solid walls, whereas the boundary conditions for the free, annular jet involve free surfaces, a transition from the no-penetration to the free-surface flow is expected. Such a transition is not considered in this paper where the interest lies in the region below the nozzle exit.

Since the flow is irrotational, the liquid pressure can be determined from Bernoulli's equation as

$$p^* = -\rho^* \frac{\partial \phi^*}{\partial t^*} - \frac{1}{2}\rho^* \left(\left(\frac{\partial \phi^*}{\partial r^*} \right)^2 + \left(\frac{\partial \phi^*}{\partial z^*} \right)^2 \right) + \rho^* g^* z^* + b^*(t^*), \tag{5}$$

where p^* denotes the pressure, ρ^* is the liquid's density, g^* is the gravitational acceleration, t^* is time, and b^* is the time-dependent Bernoulli constant. This constant can be included without loss of generality in the velocity potential since the velocity field is the gradient of the

velocity potential and only the pressure gradient appears in the Euler equations. Note that, if this is done, p^* represents the difference between the static and stagnation pressures under steady state conditions.

For long or slender, annular liquid jets, $\epsilon = R_0^*/L \ll 1$, where R_0^* and L^* denote the jet's mean radius at the nozzle exit and a characteristic axial distance, e.g., the convergence length, respectively. If the radial and axial coordinates are nondimensionalized with respect to R_0^* and L^*, respectively, the potential with respect to $u_0^* L^*$, t^* with respect to L^*/u_0^*, and the pressure with respect to $\rho^* u_0^{*2}/2$, where u_0^* is a (constant) reference axial velocity component, Eqs. (1)–(5) become, after substituting Eq. (5) into Eqs. (3) and (4),

$$\epsilon^2 \frac{\partial^2 \phi}{\partial z^2} + \frac{1}{r}\frac{\partial}{\partial r}\left(r\frac{\partial \phi}{\partial r}\right) = 0, \tag{6}$$

$$\frac{\partial \phi(R_i, z, t)}{\partial r} = \epsilon^2\left(\frac{\partial R_i}{\partial t} + \frac{\partial \phi(R_i, z, t)}{\partial z}\frac{\partial R_i}{\partial z}\right), \qquad i = 1, 2, \tag{7}$$

$$\left(\frac{\partial \phi(R_1, z, t)}{\partial r}\right)^2 = \epsilon^2\left(-\gamma_1 - 2\frac{\partial \phi(R_1, z, t)}{\partial t} - \left(\frac{\partial \phi(R_1, z, t)}{\partial z}\right)^2 + \frac{z}{Fr} + \frac{1}{We}\left(\frac{1}{R_1\left(1 + \epsilon^2(\partial R_1/\partial z)^2\right)^{1/2}} - \frac{\epsilon^2\left(\partial^2 R_1/\partial z^2\right)}{\left(1 + \epsilon^2(\partial R_1/\partial z)^2\right)^{3/2}}\right)\right), \tag{8}$$

$$\left(\frac{\partial \phi(R_2, z, t)}{\partial r}\right)^2 = \epsilon^2\left(-\gamma_2 - 2\frac{\partial \phi(R_2, z, t)}{\partial t} - \left(\frac{\partial \phi(R_2, z, t)}{\partial z}\right)^2 + \frac{z}{Fr} - \frac{1}{We}\left(\frac{1}{R_2\left(1 + \epsilon^2(\partial R_2/\partial z)^2\right)^{1/2}} - \frac{\epsilon^2\left(\partial^2 R_2/\partial z^2\right)}{\left(1 + \epsilon^2(\partial R_2/\partial z)^2\right)^{3/2}}\right)\right), \tag{9}$$

$$p = -2\frac{\partial \phi}{\partial t} - \left(\frac{1}{\epsilon^2}\left(\frac{\partial \phi}{\partial r}\right)^2 + \left(\frac{\partial \phi}{\partial z}\right)^2\right) + \frac{z}{Fr}, \tag{10}$$

where $\gamma_i = 2p_i^*/\rho^* u_0^{*2}$, $Fr = u_0^{*2}/2g^*L^*$ is the Froude number, $We = \rho^* R_0^* u_0^{*2}/2\sigma^*$ is the Weber number, and u_0^* is the average axial velocity component at the nozzle exit for inertia-dominated, annular liquid jets.

The length used to nondimensionalize the axial coordinate in this section may be replaced by $u_0^{*2}/2g^*$ which corresponds to a Froude number equal to one, and the condition of slenderness implies that $u_0^{*2}/2g^* \gg R_0^*$.

In the next paragraphs, several flow regimes for inertia-dominated, annular liquid jets are considered.

2.1 $We = \infty$ and $Fr = O(1)$

If there is no surface tension, i.e., the Weber number is infinite, and $Fr = O(1)$, the velocity potential and the jet's mean radius at the inner and outer interfaces can be written in terms of ϵ as

$$\phi = \phi_0 + \epsilon^2\phi_2 + O(\epsilon^4), \tag{11}$$

$$R_1 = R_{10} + \epsilon^2 R_{12} + O(\epsilon^4), \tag{12}$$

$$R_2 = R_{20} + \epsilon^2 R_{22} + O(\epsilon^4). \tag{13}$$

Expansion of the kinematic (Eq. (7)) and dynamic (Eqs. (8) and (9)) boundary conditions at R_1 and R_2 in Taylor's series around R_{10} and R_{20}, respectively, and substitution of Eqs. (11)–(13) into Eqs. (6)–(9) result in a system of equations in powers of ϵ^2. Equating terms of $O(\epsilon^0)$ yields

$$\frac{1}{r}\frac{\partial}{\partial r}\left(r\frac{\partial\phi_0}{\partial r}\right) = 0, \tag{14}$$

$$\frac{\partial\phi_0(R_{i0}, z, t)}{\partial r} = 0, \qquad i = 1, 2. \tag{15}$$

The solution of Eq. (14) subject to Eq. (15) is $\phi_0(z, t) = B(z, t)$. Equating terms of $O(\epsilon^2)$ yields

$$\frac{\partial^2\phi_0}{\partial z^2} + \frac{1}{r}\frac{\partial}{\partial r}\left(r\frac{\partial\phi_2}{\partial r}\right) = 0, \tag{16}$$

$$\frac{\partial\phi_2(R_{i0}, z, t)}{\partial r} + R_{i2}\frac{\partial^2\phi_0(R_{i0}, z, t)}{\partial r^2} = \frac{\partial R_{i0}}{\partial t} + \frac{\partial R_{i0}}{\partial z}\frac{\partial\phi_0(R_{i0}, z, t)}{\partial z}, \qquad i = 1, 2, \tag{17}$$

$$2\frac{\partial\phi_0(R_{i0}, z, t)}{\partial r}\left(\frac{\partial\phi_2(R_{i0}, z, t)}{\partial r} + R_{i2}\frac{\partial^2\phi_0(R_{i0}, z, t)}{\partial r^2}\right) = -\gamma_i + \frac{z}{Fr} - \left(\frac{\partial\phi_0(R_{i0}, z, t)}{\partial z}\right)^2 - 2\frac{\partial\phi_0(R_{i0}, z, t)}{\partial t}, \qquad i = 1, 2. \tag{18}$$

The solution of Eq. (16) is

$$\phi_2(r,z,t) = -\frac{B''}{4}r^2 + C\ln r + D \tag{19}$$

where the primes denote differentiation with respect to z, and C and D are functions of z and t.

Substitution of Eq. (19) into Eq. (17) yields

$$C = \frac{1}{2}\frac{\partial R_{10}^2}{\partial t} + \frac{1}{2}\frac{\partial\left(R_{10}^2 B'\right)}{\partial z} = \frac{1}{2}\frac{\partial R_{20}^2}{\partial t} + \frac{1}{2}\frac{\partial\left(R_{20}^2 B'\right)}{\partial z}, \tag{20}$$

which can be substracted to yield

$$\frac{\partial\left(R_{20}^2 - R_{10}^2\right)}{\partial t} + \frac{\partial\left(\left(R_{20}^2 - R_{10}^2\right)B'\right)}{\partial z} = 0, \tag{21}$$

which is a continuity equation.

Finally, the dynamic boundary conditions, i.e., Eq. (18), require that

$$-\gamma_i + \frac{z}{Fr} - \left(\frac{\partial B}{\partial z}\right)^2 - 2\frac{\partial B}{\partial t} = 0, \qquad i = 1,2. \tag{22}$$

Therefore, mathematical compatibility requires that $\gamma_1 = \gamma_2 = \gamma$, and

$$-\gamma + \frac{z}{Fr} - \left(\frac{\partial B}{\partial z}\right)^2 - 2\frac{\partial B}{\partial t} = 0, \tag{23}$$

which is here referred to as unsteady Torricelli's free-fall law since it coincides with Torricelli's free-law formula for steady flows.

Equating terms of $O(\epsilon^4)$ in the dynamic boundary conditions yields

$$\left(\frac{\partial\phi_2(R_{i0},z,t)}{\partial r}\right)^2 = -2\frac{\partial\phi_0(R_{i0},z,t)}{\partial z}\frac{\partial\phi_2(R_{i0},z,t)}{\partial z} - 2\frac{\partial\phi_2(R_{i0},z,t)}{\partial t}, \qquad i = 1,2, \tag{24}$$

which imply that

$$\left(-\frac{1}{2}B''R_{i0}+\frac{C}{R_{i0}}\right)^2=-2B'\left(-\frac{1}{4}B'''R_{i0}^2+C'\ln R_{i0}+D'\right)$$
$$-2\left(\frac{\partial D}{\partial t}+\frac{\partial C}{\partial t}\ln R_{i0}-\frac{R_{i0}^2}{4}\frac{\partial B''}{\partial t}\right),\qquad i=1,2. \tag{25}$$

Equations (25) can be substracted and written, after using Eq. (20), as

$$\left(\frac{\partial R_{20}}{\partial t}+B'\frac{\partial R_{20}}{\partial z}\right)^2-\left(\frac{\partial R_{10}}{\partial t}+B'\frac{\partial R_{10}}{\partial z}\right)^2$$
$$=-2B'\left(C'\ln\frac{R_{20}}{R_{10}}-\frac{1}{4}B'''\left(R_{20}^2-R_{10}^2\right)\right)$$
$$-2\frac{\partial C}{\partial t}\ln\frac{R_{20}}{R_{10}}+\frac{R_{20}^2-R_{10}^2}{2}\frac{\partial B''}{\partial t}, \tag{26}$$

which together with Eqs. (20) and (23) provide a system of partial differential equations for B', C, R_{10}, and R_{20}. Once these values are known, Eq. (25) may be used to determine D.

The pressure can be expressed as

$$p=p_0+\epsilon^2p_2+O(\epsilon^4), \tag{27}$$

which can be substituted together with Eq. (11) and the results obtained in this section into Eq. (10) to yield $p_0=\gamma$, i.e., to leading order, the pressure is uniform throughout the jet and equal to the pressure of the gases which are enclosed by and surround the annular liquid jet.

2.2. *$We=\infty$ and $Fr=O(\epsilon^{-2})$*

If there is no surface tension and $Fr=\epsilon^{-2}F$ where $F=O(1)$, the regular perturbation expansion used in the previous section yields Eqs. (14)–(23) without the terms which contain the Froude number. For example, Eq. (23) becomes

$$-\gamma-\left(\frac{\partial B}{\partial z}\right)^2-2\frac{\partial B}{\partial t}=0, \tag{28}$$

which indicates that, for steady jets, the axial velocity is uniform to leading order.

The dynamic boundary conditions to $O(\epsilon^4)$ are

$$\left(\frac{\partial\phi_2(R_{i0},z,t)}{\partial r}\right)^2 = -2\frac{\partial\phi_0(R_{i0},z,t)}{\partial z}\frac{\partial\phi_2(R_{i0},z,t)}{\partial z} - 2\frac{\partial\phi_2(R_{i0},z,t)}{\partial t} + \frac{z}{F}, \qquad i=1,2, \quad (29)$$

which imply that

$$\left(-\frac{1}{2}B''R_{i0} + \frac{C}{R_{i0}}\right)^2 = -2B'\left(-\frac{1}{4}B'''R_{i0}^2 + C'\ln R_{i0} + D'\right) - 2\left(\frac{\partial D}{\partial t} + \frac{\partial C}{\partial t}\ln R_{i0} - \frac{R_{i0}^2}{4}\frac{\partial B''}{\partial t}\right) + \frac{z}{F}, \qquad i=1,2 \quad (30)$$

which can be substracted and written as Eq. (26).

Equations (20), (26), and (28) provide a system of partial differential equations for B', C, R_{10}, and R_{20}. Once these values are known, Eq. (30) may be used to determine D. The pressure at leading order coincides with that of the previous section.

2.3. $We = O(\epsilon^{-2})$ and $Fr = O(1)$

Surface tension effects can be easily included in the perturbation method employed in the previous section. If $We = O(1/\epsilon^2)$, i.e., $We = W/\epsilon^2$ and $W = O(1)$, Eqs. (11)–(13) may be used, Eqs. (14)–(17) and (19)–(23) are still valid, while the dynamic boundary conditions to $O(\epsilon^4)$ yield

$$\left(-\frac{1}{2}B''R_{10} + \frac{C}{R_{10}}\right)^2 = -2B'\left(-\frac{1}{4}B'''R_{10}^2 + C'\ln R_{10} + D'\right) + \frac{1}{WR_{10}} - 2\left(\frac{\partial D}{\partial t} + \frac{\partial C}{\partial t}\ln R_{10} - \frac{R_{10}^2}{4}\frac{\partial B''}{\partial t}\right) \quad (31)$$

$$\left(-\frac{1}{2}B''R_{20} + \frac{C}{R_{20}}\right)^2 = -2B'\left(-\frac{1}{4}B'''R_{20}^2 + C'\ln R_{20} + D'\right) - \frac{1}{WR_{20}} - 2\left(\frac{\partial D}{\partial t} + \frac{\partial C}{\partial t}\ln R_{20} - \frac{R_{20}^2}{4}\frac{\partial B''}{\partial t}\right), \quad (32)$$

which can be substracted to yield

$$\left(\frac{\partial R_{20}}{\partial t}+B'\frac{\partial R_{20}}{\partial z}\right)^2-\left(\frac{\partial R_{10}}{\partial t}+B'\frac{\partial R_{10}}{\partial z}\right)^2$$
$$=-2B'\left(C'\ln\frac{R_{20}}{R_{10}}-\frac{1}{4}B'''\left(R_{20}^2-R_{10}^2\right)\right)-2\frac{\partial C}{\partial t}\ln\frac{R_{20}}{R_{10}}$$
$$+\frac{R_{20}^2-R_{10}^2}{2}\frac{\partial B''}{\partial t}-\frac{1}{W}\left(\frac{1}{R_{10}}+\frac{1}{R_{20}}\right). \tag{33}$$

Equation (33) reduces to Eq. (26) when $W=\infty$. Equations (20), (23), and (33) represent a system of partial differential equations which can be solved for B', C, R_{10}, and R_{20}. Once these values are known, Eq. (31) or (32) may be used to determine D.

Equations (11) and (23) and the results obtained in this section imply that, to $O(\epsilon^0)$, the pressure is uniform throughout the jet and equal to the pressure of the gases which are enclosed by and surround the annular liquid jet.

2.4. *We* $= O(\epsilon^{-2})$ *and Fr* $= O(\epsilon^{-2})$

If $We=O(1/\epsilon^2)$ and $Fr=O(1/\epsilon^2)$, i.e., $We=W/\epsilon^2$ and $Fr=F/\epsilon^2$ with $W=O(1)$ and $F=O(1)$, Eqs. (31) and (32) are to be replaced by

$$\left(-\frac{1}{2}B''R_{10}+\frac{C}{R_{10}}\right)^2=-2B'\left(-\frac{1}{4}B'''R_{10}^2+C'\ln R_{10}+D'\right)+\frac{1}{WR_{10}}$$
$$+\frac{z}{F}-2\left(\frac{\partial D}{\partial t}+\frac{\partial C}{\partial t}\ln R_{10}-\frac{R_{10}^2}{4}\frac{\partial B''}{\partial t}\right), \tag{34}$$

$$\left(-\frac{1}{2}B''R_{20}+\frac{C}{R_{20}}\right)^2=-2B'\left(-\frac{1}{4}B'''R_{20}^2+C'\ln R_{20}+D'\right)-\frac{1}{WR_{20}}$$
$$+\frac{z}{F}-2\left(\frac{\partial D}{\partial t}+\frac{\partial C}{\partial t}\ln R_{20}-\frac{R_{20}^2}{4}\frac{\partial B''}{\partial t}\right), \tag{35}$$

which can be substracted to yield Eq. (33). Equations (20, (28), and (33) can be solved to obtain B', C, R_{10}, and R_{20}.

At this point, it is important to indicate that the results of the four previous sections indicate that, if the Weber number is sufficiently large,

mathematical compatibility requires that the pressure of the gases enclosed by the annular jet be identical to that of the gases surrounding the jet and identical to the liquid's pressure. Therefore, the results presented in Subsections 2.1–2.4 are consistent with a hydraulic approximation to leading order in that the liquid's pressure is uniform throughout the jet. Furthermore, Eqs. (26) and (33) indicate that, in addition to $B(0,t)$, $R_{10}(0,t)$, and $R_{20}(0,t)$, an additional boundary condition must be provided. Such a boundary condition may be the specification of either $\partial R_{10}(0,t)/\partial z$ or $\partial R_{20}(0,t)/\partial z$ since these partial derivatives are related through Eq. (21).

In order to handle a pressure difference between the gases enclosed by and surrounding the annular jet, surface tension effects must be much larger than those considered in the previous sections as indicated in the next section.

2.5. *We* = *O*(1) *and Fr* = *O*(1)

If $We = O(1)$, and $Fr = O(1)$, Eqs. (11)–(13) may be used to obtain Eqs. (14)–(17), while the terms $1/WeR_{10}$ and $-1/WeR_{20}$ must be added to the right hand sides of Eq. (18) for $i = 1$ and 2, respectively. Furthermore, Eq. (18) becomes

$$-\gamma_1 + \frac{z}{Fr} - \left(\frac{\partial B}{\partial z}\right)^2 - 2\frac{\partial B}{\partial t} + \frac{1}{WeR_{10}} = 0, \tag{36}$$

$$-\gamma_2 + \frac{z}{Fr} - \left(\frac{\partial B}{\partial z}\right)^2 - 2\frac{\partial B}{\partial t} - \frac{1}{WeR_{20}} = 0. \tag{37}$$

Equations (36) and (37) can be substracted and added to yield, respectively,

$$\gamma_1 - \gamma_2 = \frac{1}{We}\left(\frac{1}{R_{10}} + \frac{1}{R_{20}}\right), \tag{38}$$

$$-\frac{\gamma_1 + \gamma_2}{2} + \frac{z}{Fr} - (B')^2 - 2\frac{\partial B}{\partial t} + \frac{1}{2We}\left(\frac{1}{R_{10}} - \frac{1}{R_{20}}\right) = 0. \tag{39}$$

Equation (38) indicates that the difference between the pressure of the gases enclosed by and those surrounding the annular liquid jet is balanced by surface tension effects, whereas Eq. (39) shows the effect of surface tension on the leading order axial velocity component.

Equations (20), (38), and (39) may be solved to obtain the values of B', C, R_{10}, and R_{20}. Furthermore, it must be indicated that, for $We = O(1)$, closure of the equations at leading order is achieved without invoking the

dynamic boundary conditions at $O(\epsilon^4)$, while the analysis presented in Subsections 2.1–2.4 required these boundary conditions.

2.6. *We* = $O(1)$ *and* *Fr* = $O(\epsilon^{-2})$

If $We = O(1)$ and $Fr = F\epsilon^{-2}$ where $F = O(1)$, it may be easily shown that the equations governing the flow are Eqs. (20), (38), and

$$-\frac{\gamma_1 + \gamma_2}{2} - (B')^2 + \frac{1}{2We}\left(\frac{1}{R_{10}} - \frac{1}{R_{20}}\right) - 2\frac{\partial B}{\partial t} = 0. \qquad (40)$$

Equation (40) indicates that gravity does not affect the flow at leading order, and Eqs. (20), (38), and (40) may be solved to obtain the values of B', C, R_{10}, and R_{20}.

Since a large surface tension implies that the Weber number is small and since the Weber number is the ratio of a characteristic axial velocity at the nozzle exit, u_0^*, to the capillary velocity, $u_c^* = (\sigma^*/\rho^* R_0^*)^{1/2}$, a small Weber number implies that the capillary velocity is larger than that at the nozzle exit. Therefore, asymptotic analyses of large surface tension, i.e., capillary, annular jets may be conveniently performed by nondimensionalizing the liquid's axial velocity with respect to the capillary velocity as indicated in the next section.

3. UNSTEADY, SLENDER, CAPILLARY, ANNULAR LIQUID JETS

If the axial and radial coordinates, potential, jet's radii and pressure with respect to L^*, R_0^*, $u_c^* L^*$, R_0^*, and $\rho^* u_c^{*2}/2$, respectively, so that Eqs. (1)–(5) become Eqs. (6), (7), and

$$\left(\frac{\partial \phi(R_1, z, t)}{\partial r}\right)^2 = \epsilon^2\left(-\gamma_1 - \left(\frac{\partial \phi(R_1, z, t)}{\partial z}\right)^2 - 2\frac{\partial \phi(R_1, z, t)}{\partial t}\right.$$

$$\left. + \frac{zBo}{\epsilon} + \frac{1}{R_1\left(1 + \epsilon^2(\partial R_1/\partial z)^2\right)^{1/2}} - \frac{\epsilon^2\left(\partial^2 R_1/\partial z^2\right)}{\left(1 + \epsilon^2(\partial R_1/\partial z)^2\right)^{3/2}}\right) \qquad (41)$$

$$\left(\frac{\partial \phi(R_2, z, t)}{\partial r}\right)^2 = \epsilon^2\left(-\gamma_2 - \left(\frac{\partial \phi(R_2, z, t)}{\partial z}\right)^2 - 2\frac{\partial \phi(R_2, z, t)}{\partial t}\right.$$

$$\left. + \frac{zBo}{\epsilon} - \frac{1}{R_2\left(1 + \epsilon^2(\partial R_2/\partial z)^2\right)^{1/2}} + \frac{\epsilon^2\left(\partial^2 R_2/\partial z^2\right)}{\left(1 + \epsilon^2(\partial R_2/\partial z)^2\right)^{3/2}}\right) \qquad (42)$$

$$p = -\left(2\frac{\partial \phi}{\partial t} + \frac{1}{\epsilon^2}\left(\frac{\partial \phi}{\partial r}\right)^2 + \left(\frac{\partial \phi}{\partial z}\right)^2\right) + \frac{zBo}{\epsilon}, \tag{43}$$

where $Bo = 2\rho^* g^* R_0^{*2}/\sigma^*$ is the Bond number.

If $Bo = \hat{B}\epsilon$, where $\hat{B} = O(1)$, substitution of Eqs. (11)–(13) into Eqs. (6), (7), (41), and (42) and expansion of the interface boundary conditions in Taylor's series yield Eqs. (20) and (21), while Eqs. (41) and (42) become to $O(\epsilon^2)$

$$-\gamma_1 + z\hat{B} - \left(\frac{\partial B}{\partial z}\right)^2 - 2\frac{\partial B}{\partial t} + \frac{1}{R_{10}} = 0, \tag{44}$$

$$-\gamma_2 + z\hat{B} - \left(\frac{\partial B}{\partial z}\right)^2 - 2\frac{\partial B}{\partial t} - \frac{1}{R_{20}} = 0. \tag{45}$$

Equations (44) and (45) can be substracted and added to yield, respectively,

$$\gamma_1 - \gamma_2 = \frac{1}{R_{10}} + \frac{1}{R_{20}}, \tag{46}$$

$$-\frac{\gamma_1 + \gamma_2}{2} + z\hat{B} - (B')^2 - 2\frac{\partial B}{\partial t} + \frac{1}{2}\left(\frac{1}{R_{10}} - \frac{1}{R_{20}}\right) = 0. \tag{47}$$

Equation (46) indicates that the difference between the pressure of the gases enclosed by and those surrounding the annular liquid jet is balanced by surface tension effects, whereas Eq. (47) shows the effect of surface tension on the leading order axial velocity component. Equations (20), (46), and (47) may be solved to obtain the values of B', C, R_{10}, and R_{20}.

If $Bo = \hat{B}\epsilon^3$, where $\hat{B} = O(1)$, Eq. (47) is to be replaced by

$$-\frac{\gamma_1 + \gamma_2}{2} - (B')^2 - 2\frac{\partial B}{\partial t} + \frac{1}{2}\left(\frac{1}{R_{10}} - \frac{1}{R_{20}}\right) = 0, \tag{48}$$

which together with Eqs. (20) and (46) may be solved to obtain the values of B, R_{10}, and R_{20}.

4. STEADY, SLENDER, ANNULAR LIQUID JETS

For steady annular liquid jets, the equations presented in Subsections 2.1–2.6 have analytical solutions which are obtained in the next paragraphs. For the sake of convenience, the following definition will be adopted $B' = U$.

Under steady state conditions, the solutions of Eqs. (21) and (22) can be written as

$$U\frac{R_{20}^2 - R_{10}^2}{2} = \beta, \qquad U = \left(1 + \frac{z}{H}\right)^{1/2}, \tag{49}$$

where β denotes the volumetric flow rate and $-\gamma$ has been set to one.

Equations (20) and (26) and Eqs. (20) and (33) may be compactly written as

$$\psi' = C, \tag{50}$$

$$\psi'' = \frac{\beta JU'' - (U/2)^{1/2}\left(\psi^{-1/2} + (\psi+\beta)^{-1/2}\right) - JU^2\left((R'_{20})^2 - (R'_{10})^2\right)}{JU\ln((\psi+\beta)/\psi)}, \tag{51}$$

$$R_{10} = \left(\frac{2\psi}{U}\right)^{1/2}, \qquad R_{20} = \left(\frac{2(\psi+\beta)}{U}\right)^{1/2}. \tag{52}$$

where

$$\psi = \frac{1}{2}UR_{10}^2, \tag{53}$$

and $(H, J) = (Fr, \infty)$, (∞, ∞), (Fr, W), and (∞, W) for the equations presented in Subsections 2.1–2.4, respectively, under steady state conditions.

Equations (50)–(52) may be solved numerically by means of, for example, a fourth-order accurate Runge–Kutta method, to obtain the values of ψ, R_{10}, and R_{20}.

The steady state equations corresponding to Subsections 2.5 and 2.6 may be compactly written as Eq. (49a) and

$$\gamma_1 - \gamma_2 = \frac{1}{We}\left(\frac{1}{R_{10}} + \frac{1}{R_{20}}\right), \tag{54}$$

$$-\frac{\gamma_1 + \gamma_2}{2} + \frac{z}{H} - U^2 + \frac{1}{2We}\left(\frac{1}{R_{10}} - \frac{1}{R_{20}}\right) = 0, \tag{55}$$

which can be combined to yield the following algebraic equation for R_{10}

$$-\frac{\gamma_1 + \gamma_2}{2} + \frac{z}{H} - \left(\frac{2\beta\left(WeR_{10}(\gamma_1 - \gamma_2) - 1\right)}{R_{10}}\right)^2 \frac{1}{1 - \left(WeR_{10}(\gamma_1 - \gamma_2) - 1\right)^2} + \frac{1}{2We}\left(\frac{2}{R_{10}} - We(\gamma_1 - \gamma_2)\right) = 0, \tag{56}$$

where $H = Fr$ and ∞ for the flow regimes considered in Subsections 2.5 and 2.6, respectively.

The steady state solutions of the capillary, annular liquid jets presented in Section 3 can be obtained in an analogous manner to those of Eqs. (54)–(56), and are not presented here.

5. PRESENTATION OF RESULTS

Some sample results illustrating the shape of steady, annular liquid jets are presented in Figs. 1 and 2 which correspond to upward and downward, respectively, annular liquid jets. The results presented in these figures were obtained by solving the ordinary differential equations of Section 4 by means of a fourth-order accurate Runge–Kutta method.

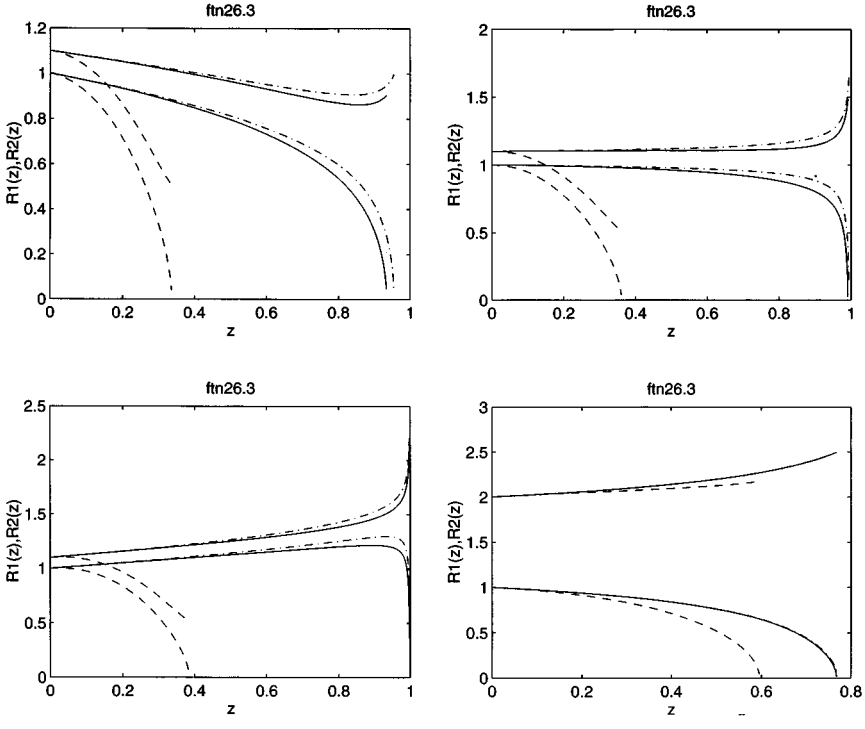

FIG. 1. Shapes of upward, annular liquid jets. ($Fr = -1$; $R_{10}(0) = 1$; $We = \infty$ (dashed-dotted lines), 1 (dashed lines), 100 (solid lines); top left, $R'_{10}(0) = -0.25$ and $R_{20}(0) = 1.10$; top right, $R'_{10}(0) = 0$ and $R_{20}(0) = 1.10$; bottom left, $R'_{10}(0) = 0.25$ and $R_{20}(0) = 1.10$; bottom right, $R'_{10}(0) = 0$ and $R_{20}(0) = 2$).

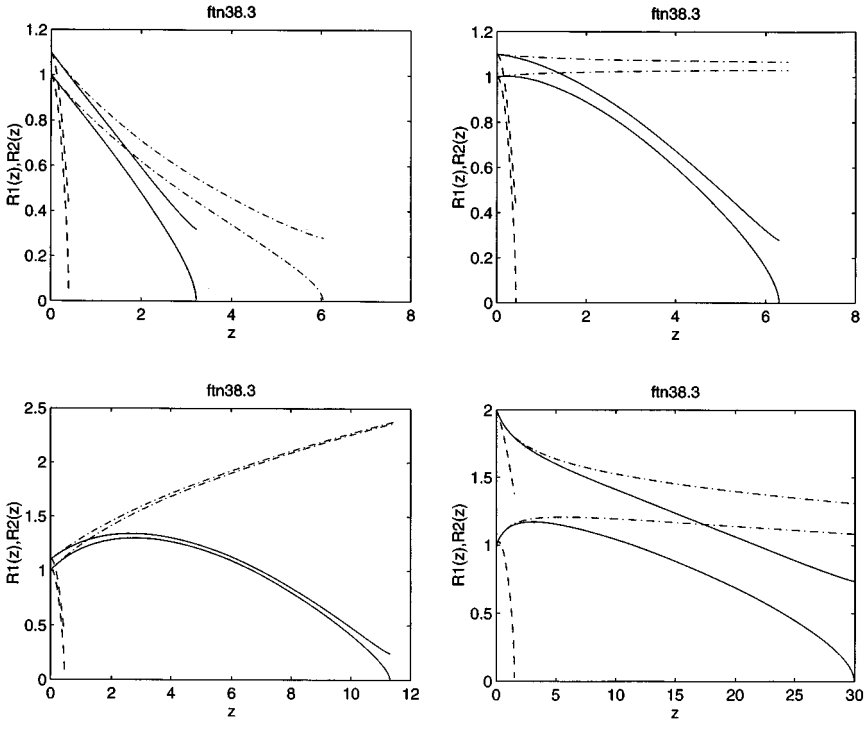

FIG. 2. Shapes of downward, annular liquid jets. ($Fr = 1$; $R_{10}(0) = 1$; $We = \infty$ (dashed-dotted lines), 1 (dashed lines), 100 (solid lines); top left, $R'_{10}(0) = -0.25$ and $R_{20}(0) = 1.10$; top right, $R'_{10}(0) = 0$ and $R_{20}(0) = 1.10$; bottom left, $R'_{10}(0) = 0.25$ and $R_{20}(0) = 1.10$; bottom right, $R'_{10}(0) = 0$ and $R_{20}(0) = 2$).

Figure 1 indicates that the convergence length increases as the Weber number and the nozzle exit angle are increased. Note that according to the analysis presented in Section 4, the axial velocity of the liquid is identically equal to zero at $z = -Fr$, and that the jet's thickness increases as this height is approached.

Figure 1 (bottom right) shows that the convergence length decreases as the jet's thickness at the nozzle exit is increased for $We = 100$ and $We = \infty$, while the opposite behaviour is observed for $We = 1$.

Figure 2 illustrates the shape of downward, annular liquid jets and shows that the convergence length increases as the Weber number and the nozzle exit angle are increased and that the jet's thickness first decreases from its value at the nozzle exit and then it increases as the convergence point is approached. Figure 2 also shows the jet's contraction at the nozzle exit. Furthermore, the annular jet corresponding to $We = \infty$ did not converge onto the symmetry axis for $R'_{10} = 0$ and 0.25 and $z \leq 100$.

Figure 2 (bottom right) shows that the convergence length decreases as the jet's thicknesses at the nozzle exit is increased for $We = 100$ and $We = \infty$, while the opposite behaviour is observed for $We = 1$.

6. CONCLUSIONS

Perturbation methods have been used to analyze the fluid dynamics of steady and unsteady, slender, inviscid, incompressible, irrotational, axisymmetric, annular liquid jets. Two flow regimes corresponding to inertia- and capillarity-dominated annular liquid jets have been identified. The first regime is controlled by the Froude and Weber numbers, while the second one depends on the Bond number. It has been shown that, for large Weber numbers, the determination of the velocity potential at leading order requires the dynamic boundary conditions at the jet's interfaces at fourth-order in the slenderness ratio, whereas, in the capillary regime, the velocity potential at leading order is determined from leading order equations.

ACKNOWLEDGMENTS

The research reported in this paper was supported by Project PB94-1494 from the D.G.I.C.Y.T. of Spain, The author is grateful to The Centro Europeo de Paralelismo de Barcelona (CEPBA), Spain, where some of the computations presented here were performed on a CONVEX C3480 supercomputer.

REFERENCES

1. M. Boussinesq, Théorie des expériences de Savart, sur la forme que prend une veine liquide après s'être choquée contre un plan circulaire, *C.R. Acad. Sci. Paris* **69** (1869), 45–48.
2. M. Boussinesq, Théorie des expériences de Savart sur la forme que prend une veine liquide après s'être heurtée contre un plan circulaire, *C.R. Acad. Sci. Paris* **69** (1869), 128–131.
3. G. N. Lance and R. L. Perry, Water bells, *Proc. Phys. Soc.* (*London*) *Ser. B* **66** (1953), 1067–1072.
4. F. L. Hopwood, Water bells, *Proc. Phys. Soc.* (*London*) *Ser. B* **65** (1952), 2–5.
5. G. I. Taylor, The dynamics of thin sheets of fluid. Part I. Water bells, *Proc. Roy. Soc. London Ser. A* **253** (1959), 289–295.
6. M. H. I. Baird and J. F. Davidson, Annular jets. I. Fluid dynamics, *Chem. Engrg. Sci.* **17** (1962), 467–472.
7. A. M. Binnie and H. B. Squire, Liquid jets of annular cross-section, *The Engineer* (*London*) **171** (1941), 236–238.

8. J. H. Dumbleton, Effect of gravity on the shape of water bells, *J. Appl. Phys*. **40** (1969), 3950–3954.
9. M. A. Hoffman, R. K. Takahashi, and R. D. Monson, Annular liquid jet experiments, *ASME J. Fluids Engrg*. **102** (1980), 344–349.
10. J. I. Ramos, Liquid curtains. I. Fluid mechanics, *Chem. Engrg. Sci*. **43** (1988), 3171–3184.
11. J. I. Ramos, Annular liquid jets: Formulation and steady state analysis, *Z. Angew. Math. Mech*. **72** (1992), 565–589.
12. N. Chigier, J. I. Ramos, and K. Kihm, Experimental and theoretical studies of vertical annular liquid jets, *in* ''Proceedings of the Sixth Symposium on Energy Engineering Sciences: Flow and Transport in Continua,'' pp. 18–25, U.S. Department of Energy, Argonne National Laboratory, Argonne, IL, 1988.